

Optical phase measurements in red blood cells using low-coherence spectroscopy

Itay Shock^a, Alexander Barbul^b, Pinhas Girshovitz^a, Uri Nevo^a,
Rafi Korenstein^b, Natan T. Shaked^{*a}.

^a Department of Biomedical Engineering, Faculty of Engineering, Tel Aviv University,
Tel Aviv 69978, Israel.

^b Department of Physiology-Pharmacology, Faculty of Medicine, Tel Aviv University,
Tel Aviv 69978, Israel.

Abstract

We demonstrate the use of a low-coherence spectral-domain phase microscopy (SDPM) system for accurate quantitative phase measurements in red blood cells (RBCs) for the prognosis and monitoring of disease conditions that affect the visco-elastic properties of RBCs. Using the system, we performed time-recordings of cell membrane fluctuations, and compared the nano-scale fluctuation dynamics of healthy and glutaraldehyde-treated RBCs. Glutaraldehyde-treated RBCs possess a lower amplitude of fluctuations reflecting an increased membrane stiffness. To demonstrate the ability of our system to measure fluctuations of lower amplitudes than those measured by the commonly used holographic phase microscopy techniques, we also constructed a wide-field digital interferometric microscope and compared the performances of the two systems. Due to its common-path geometry, the optical-path-delay stability of SDPM was found to be less than 0.3nm in liquid environment, at least three times better than in holographic phase microscopy under the same conditions. In addition, due to the compactness of SDPM and its inexpensive and robust design, the system possesses a high potential for clinical applications.

1. INTRODUCTION

Retrieving quantitative phase information from living, unstained biological samples have given insights to the dynamic mechanisms in cells. Unlike conventional differential interference contrast (DIC) or phase contrast microscopy, which are inherently qualitative, quantitative phase microscopy allows measuring optical path delay (OPD) and topographic data of single point or full-field images¹⁻⁵.

Since red blood cells (RBCs) lack intracellular organelles, a constant index of refraction can be assumed on the entire cell's viewable area. Therefore, the RBC OPD profile measured by quantitative phase microscopy is proportional to the thickness profile of the RBC⁶. Using the time-dependent thickness profile of the RBC, cell stiffness properties can be calculated⁷. Thus, quantitative phase microscopy yields biologically-relevant parameters on live RBCs and can be used as a powerful tool for research and diagnosis.

The elastic properties of RBCs, defining their deformability, are dependent on the bending and shearing properties of the cell membrane, which are governed mostly by metabolically regulated coupling between the lipid bilayer and the underlying spectrin-actin cytoskeletal network⁸⁻¹⁰. This deformability is vital as it enables the RBC to squeeze through the small capillaries that are only several micrometers in size. Certain pathological conditions in RBCs such as

* nshaked@tau.ac.il; phone/fax +972 3 640 7100; www.tau.ac.il/~nshaked/

spherocytosis, malaria, and sickle cell disease impact the flexibility of the cells as well as change their dynamic behavior and might hinder the transportation of oxygen in the blood circulation. These effects were previously studied using qualitative and quantitative techniques^{7,8}.

Optical coherence microscopy (OCM)¹¹ is an imaging technique that is capable of recording the amplitude and phase information of the light that has interacted with an individual cell. A typical OCM system records the interference pattern between the light that has interacted with the sample and a reference wave, where the light source used is a low coherent source.

Full-field interferometric measurements of RBCs is frequently based on the principles of digital holographic microscopy¹²⁻¹⁵. In this technique, spatial interferograms are collected from an area which includes many points. These interferograms are processed into the time-dependent, two-dimensional phase profiles of the sample, which is suitable for recording both spatially-dependent and time dependent phenomena. However, digital holographic microscopy uses separate interferometer arms yielding higher degree of noise, or requires several frames of acquisition for each instance of the sample, which is not suitable for highly-dynamic samples. In addition, the energy of the light source is spread over a large area further reducing the signal to noise (SNR) ratio. Therefore, this full-field interferometric technique has inherently lower SNR compared to a single-point interferometric technique.

In single-point interferometric measurements of live cells^{16,18} the light is focused on a small area and therefore higher irradiance allows for ultrafast acquisition times with compact and reasonable-price detectors. Furthermore, single point measurements also allow for an easy-to-implement common-path geometry and a compact and portable fiber optics configuration, and thus can work even without using floating optical tables, which has a significantly-higher potential for clinical applications.

We presented a spectral-domain phase microscopy (SDPM) system¹⁹, which is based on an OCM principle, to realize a compact, portable and yet high-accuracy technique for quantitatively measuring the RBC membrane dynamics, with the potential for future clinical applications of high-accuracy blood screening. For the first time to our knowledge, we experimentally demonstrate the SDPM ability to measure RBCs with decreased amplitude of vibrations, demonstrating the superior properties of SDPM compared to a full-field interferometric technique.

2. SDPM PRINCIPLES

Schematic of the SDPM system is shown in Figure 1. A superluminescent diode (SLD) (Superlum, Inc, central wavelength 840nm, FWHM spectrum width of 50nm, 15mW fiber output power) light passes through a polarization controller and is split using a 50/50 fiber coupler. One of the outputs from the coupler is collimated and focused onto the sample using a 40× 0.66-NA microscope objective. The sample is placed in a closed chamber such that the reflection from the upper surface of the chamber is used as the reference beam and the light passing through the media and the RBC is reflected from the bottom surface and is used as the sample beam. To increase the bottom surface reflection and thus improve the SNR, the bottom surface was coated with a chrome layer for adhesion followed by a thin layer of gold for creating a reflective surface, using sputter deposition method. The combined reference and sample beams pass back through the fiber coupler to a compact spectrometer (Ocean Optics HR2000+, 2048 pixel CCD, spectral range 650nm, best efficiency 650-1100nm) where the interference pattern is recorded. As shown in Figure 1, to be able to locate object of interest, a compact digital camera arm was added to the system. The camera displays the SLD beam and the sample brightfield image simultaneously and allows the correct positioning of the SLD beam over the sample.

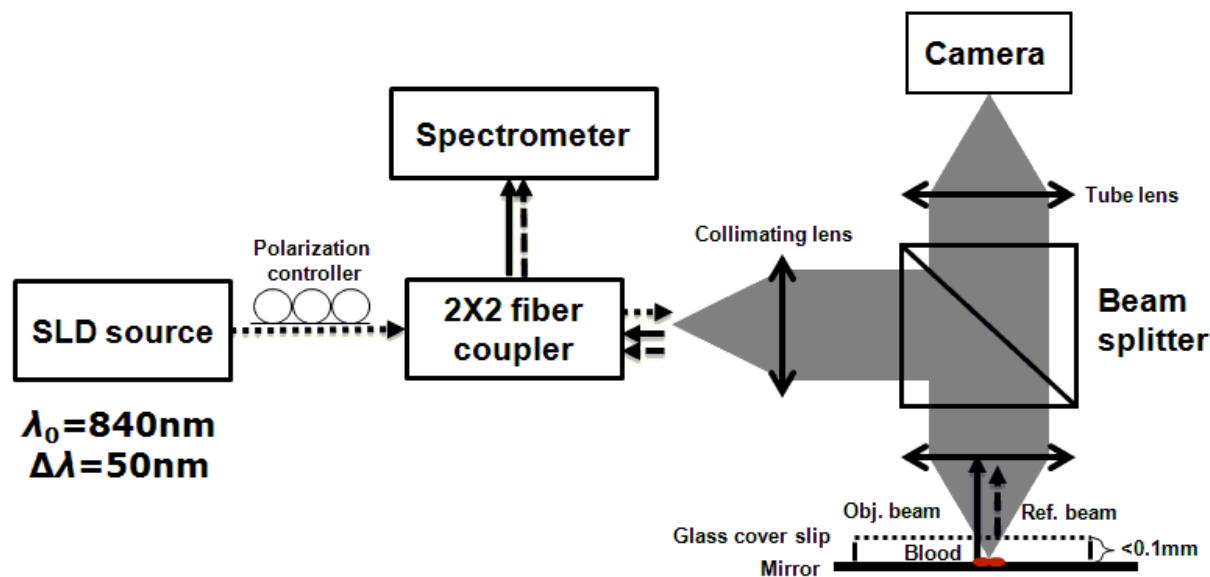


Figure 1. Schematics of the SDPM system. The blood sample is encapsulated between two partially-reflecting surfaces.

To retrieve the phase information, we used the windowed Fourier transform method^{16,20-22}. In phase measurements with Fourier domain OCM, the oscillations of the fringes in spectral domain due to OPD between the reference and sample beams are detected. Since the phase oscillates 2π rad at every shift of half a wavelength of the OPD, high-sensitivity phase measurements of the fringes can provide an ultrahigh-accuracy measurement of the change in the OPD¹⁶.

3. EXPERIMENTAL METHODS

To demonstrate the system ability to measure live-cell fluctuations, we used glutaraldehyde-treated RBCs at various concentration levels. Glutaraldehyde causes cross-linking of proteins and destroys the lipid membrane, leading to an altered structure and thus affecting the RBC membrane elasticity characteristics¹⁷. By inducing low-membrane fluctuations, we demonstrated that our system is more sensitive than commonly-used quantitative phase measurement systems, such as ones that are based on wide-field digital interferometry.

3.1 SDPM system

We constructed the system shown in Figure 1 and described in Section 2. To measure the time behavior of the RBC using SDPM, the SLD beam was focused on the highest point of the cell torus, located approximately half way between the outer cell rim and the cell center. Spectral data was collected at 20 Hz with an integration time of 1ms for a period of 30 seconds. To receive the membrane displacement h , the OPD is divided by the index of refraction difference, between the media and the RBC:

$$h = \frac{OPD}{\Delta n} , \quad (1)$$

where Δn is the difference in the index of refraction between the RBC and the surrounding media. Index of refraction was assumed 1.395 for the RBC and 1.33 for the media.

On a non floating table, the SDPM system has remarkable OPD stability in liquid environment of 690 pm. This stability is better than the stability achieved with the WFDI even on a floating table. Thus the SDPM system has a great potential for use outside the optical labs. On an isolated floating optical table the SDPM had an OPD stability of 300pm.

3.2 WFDI system

The WFDI setup is based on Mach-Zander interferometer²³. The two systems (SDPM and WFDI) were built on the same table. For WFDI, phase measurements data was collected simultaneously from a region containing several RBCs. The system produces a phase image with field of view of $73\mu\text{m} \times 63\mu\text{m}$ at 20Hz and 1ms exposure time for 30 seconds. Data was spatially averaged using a 2-D Gaussian to obtain a similar lateral resolution as that of the SDPM system. Data was taken in each RBC from a region of approximately the same area size as that of the SLD beam at about half way between the outer cell rim and the cell center. The membrane displacement h is found using Eq. (1).

3.3 RBC preparations

Fresh human blood was obtained from healthy volunteers by a fingerprick. The blood was diluted by phosphate buffered saline without Ca and Mg, supplemented with 10mM glucose (PBSG solution) and RBCs were separated by centrifugation at 1000rpm for 10 minutes at 4°C. After removing of buffy coat, RBCs were washed twice with PBSG at 2000rpm for 3 minutes. The cells were then resuspended in PBSG solution supplemented with 0.9mM CaCl₂, 0.5mM MgCl₂ and 1mg/ml bovine serum albumin. RBC suspension was then introduced into the experimental chamber, placed on the mirror-coated slide and left for 15 minutes to allow adhesion of the cells to the gold surface. Afterwards, the cells in the chamber were washed with PBSG and examined by SDPM or WFDI. Alternatively, the solution in the chamber after washing the cells with PBSG was exchanged with PBSG solution containing 1mM ethylene glycol tetraacetic acid and glutaraldehyde at 5 different concentrations of: 0.001%, 0.0025, 0.005%, 0.025%, and 2.5%. After 15 minutes of incubation at room temperature the cells in the chamber were washed with the PBSG solution to remove glutaraldehyde from the bath solution.

4. MEASUREMENTS AND RESULTS

In both systems, data was collected from 10 RBCs taken in each one of the 6 glutaraldehyde concentrations. During measurements the temperature was monitored and maintained at $22\pm 0.5^\circ\text{C}$. To determine system OPD stability, signal from an area outside the cells containing media only was recorded in each of the concentrations for 30 seconds. The membrane flickering is gradually decreased at higher concentrations of glutaraldehyde, as could be expected, due to the bonding of proteins on the membrane surface and the gradual destruction of the spectrin structure.

The standard deviation (STD) of the membrane fluctuations over 30 seconds was calculated for each RBC. As shown in Figure 2, both systems show similar membrane displacement behavior at the lower concentration levels of glutaraldehyde. For normal RBCs, the mean membrane displacement was found to be approximately $35\pm 15\text{nm}$. As the concentration levels of glutaraldehyde increase, the mean displacement decreases: $31\pm 15\text{nm}$ at 0.001%, $28\pm 8\text{nm}$ at 0.0025%, $24\pm 12\text{nm}$ at 0.005%, and $18\text{nm}\pm 8\text{nm}$ at 0.025%. At the 0.005% concentration level, about 50% of the RBC showed acanthocyte morphology. Some of the RBC displacements were just above the measurable levels of the WFDI at 15 nm mean displacement.

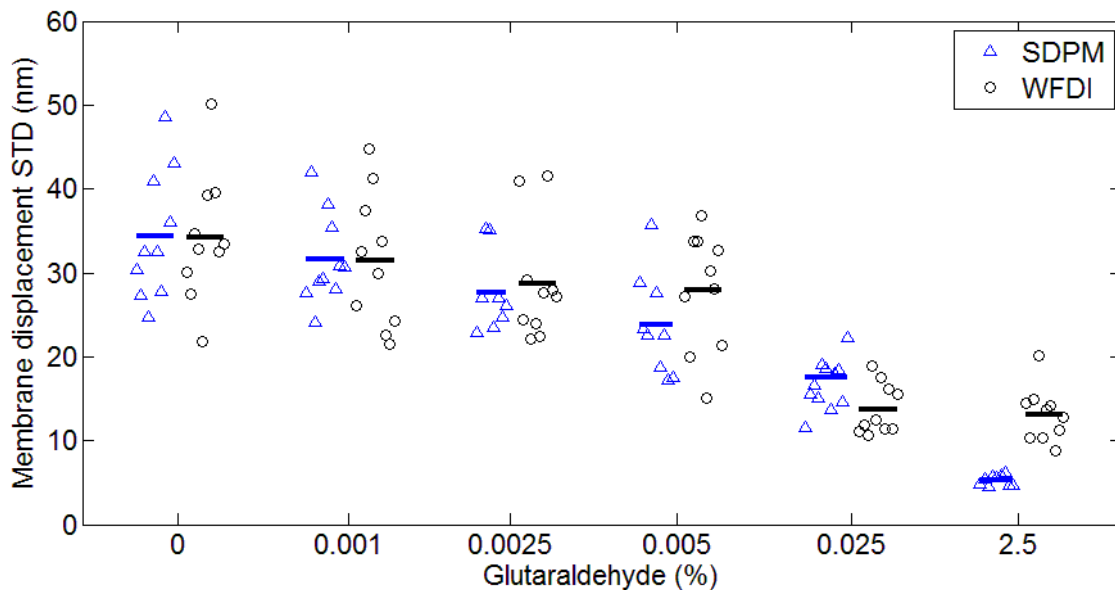


Figure 2. Membrane displacement values of ten RBCs from both systems (SDPM and WFDI) for different glutaraldehyde concentrations. Each shape represents a single cell membrane displacement STD over a 30-second time period. The horizontal line is the average value of the displacement at each concentration.

At 2.5% concentration, the RBC membrane fluctuation amplitude further decreased so that OPD measurements on these cells and the measurements on an area with media only were similar. The SDPM had OPD stability of about 300pm (about 4.5nm membrane displacement) compared to 900pm (about 14nm membrane displacement) for the WFDI system. SDPM was sensitive enough to detect fluctuations at the 0.025% glutaraldehyde concentration. WFDI, however, was not capable to detect those fluctuations due to lower sensitivity levels than the SDPM system.

These results demonstrate how elasticity changes in the membrane of RBCs manifest in temporal behavior changes. Analyzing these changes clearly shows a difference between healthy RBCs and glutaraldehyde-treated RBCs. These changes were well recorded with both systems up to 0.005% concentration with similar results. The membrane displacements, even as low as 18nm at 0.025% concentration were at least three times higher than the minimum detectable displacement of the SDPM system, whereas these displacements were just at the detectable threshold of the WFDI system. The higher degree of SNR in the SDPM system is expected to enable measuring lower membrane fluctuations characterizing various diseases such as sickle cell anemia²⁴ and malaria⁶.

5. CONCLUSION

We presented the SDPM, a simple, compact, and low-cost quantitative phase measurement technique with 0.3nm OPD sensitivity at high frame rates in a liquid environment. The sensitivity surpassed that of WFDI-based quantitative phase measurement technique by a factor of ~3 under the same experimental conditions. In spite of the fact that multiple points of measurement can be provided by WFDI, the higher-sensitivity single point measurements that can be provided by the more-compact SDPM system might be enough for diagnosis purposes. In addition, the stability of the SDPM system due to its common-path geometry means that it can be built on a non-floating table. Furthermore, the reflection geometry as well as its compactness and portability give the proposed system a high potential for clinical applications.

REFERENCES

1. Stephens, D. J., Allan, V. J., "Light microscopy techniques for live cell imaging," *Science* 300, 82-86 (2003)
 2. Yang, C., Wax, A., Hahn, M. S., Badizadegan, K. R., Dasari, R., and Feld, M. S., "Phase-referenced interferometer with subwavelength and subhertz sensitivity applied to the study of cell membrane dynamics," *Opt. Lett.* 26, 1271-1273 (2001).
 3. Choma, M. A., Yang, A. K. C., Creazzo, T. L., and Izatt, J. A., "Spectral-domain phase microscopy," *Opt. Lett.* 30, 1162-1164 (2005).
 4. Shaked, N. T., Rinehart, M. T., and Wax, A., "Dual-interference-channel quantitative-phase microscopy of live cell dynamics," *Opt. Lett.* 34, 767-769 (2009).
 5. Wang, Z., Millet, L., Mir, M., Ding, H., Unarunotai, S., Rogers, J., Gillette, M. U., and Popescu, G., "Spatial light interference microscopy (SLIM)," *Opt. Express* 19, 1016-1026 (2011).
 6. Park, Y., Silva, M. D., Popescu, G., Lykotrafitis, G., Choi, W., Feld, M. S., and Suresh, S., "Refractive index maps and membrane dynamics of human red blood cells parasitized by *Plasmodium falciparum*," *PNAS* 105, 13730-13735 (2008).
 7. Popescu, G., Park, Y., Choi, W., Dasari, R. R., Feld, M. S., and Badizadegan, K., "Imaging red blood cell dynamics by quantitative phase microscopy," *Blood Cells, Molecules and Diseases* 41, 10-16 (2008).
 8. Tuvia, S., Levin, S., Bitler, A., and Korenstein, R., "Mechanical fluctuations of the membrane-skeleton are dependent on F-Actin ATPase in human erythrocytes," *Journal of Cell Biology* 141(7), 1551-1561 (1998).
 9. Lin, L. C.-L., Gov, N., and Brown, F. L. H., "Nonequilibrium membrane fluctuations driven by active proteins," *J. Chem. Phys.* 124, 074903 (2006).
 10. Zeman, K., Engelhard, H., and Sackmann, E., "Bending undulations and elasticity of the erythrocyte membrane: effects of cell shape and membrane organization," *European Biophysics Journal* 18, 203-219 (1990).
 11. Wolfgang Drexler, [Theory of Optical Coherence Tomography], Springer, 47-72 (2008).
 12. Rappaz, B., Barbul, A., Hoffmann, A., Boss, D., Korenstein, R., Depeursinge, C., Magistretti, P. J., and Marquet, P., "Spatial analysis of erythrocyte membrane fluctuations by digital holographic microscopy," *Blood cells molecules diseases* 42, 228-232 (2009).
 13. Bernhardt, I., Ivanova, L., Langehanenberg, P., Kemper, B., and Von Bally, G., "Application of digital holographic microscopy to investigate the sedimentation of intact red blood cells and their interaction with artificial surfaces," *Bioelectrochemistry Amsterdam Netherlands* 73, 92-96 (2008).
 14. Liu, R., Dey, D. K., Boss, D., Marquet, P., and Javidi, B., "Recognition and classification of red blood cells using digital holographic microscopy and data clustering with discriminant analysis," *Journal of the Optical Society of America A* 28, 1204-1210 (2011).
 15. Ding, H., and Popescu, G., "Instantaneous spatial light interference microscopy," *Optics Express* 18, 1569-1575 (2010).
 16. Choma, M. A., Ellerbee, A. K., Yang, C., Creazzo, T. L., and Izatt, J. A., "Spectral-domain phase microscopy," *Optics Letters* 30, 1162-1164 (2005).
 17. Shin, S., Hou, J. X., Suh, J. S., Singh, M., "Validation and application of a microfluidic ektacytometer (RheoScan-D) in measuring erythrocyte deformability," *Clin. Hemorheol. Microcirc.* 37, 319-28 (2007).
 18. Verma, Y., Nandi, P., Rao, K. D., Sharma, M., and Gupta, P. K., "Use of common path phase sensitive spectral domain optical coherence tomography for refractive index measurements," *Applied Optics* 50, E7-E12 (2011).
 19. Shock, I., Barbul, A., Girshovitz, P., Nevo, U., Korenstein, R., Shaked, N.T., "Optical phase nanoscopy in red blood cells using low-coherence spectroscopy," submitted to *Journal of Biomedical Optics* (2011).
 20. Zhang, J., Rao, B., Yu, L., and Chen, Z., "High-dynamic-range quantitative phase imaging with spectral domain phase microscopy," *Opt. Lett.* 34, 3442-3444 (2009).
 21. Debnath, S. K., and Kothiyal, M. P., "Improved optical profiling using the spectral phase in spectrally resolved white-light interferometry," *Applied Optics* 45, 6965-6972 (2006).
 22. Debnath, S. K., Kothiyal, M. P., and Kim, S.-W., "Evaluation of spectral phase in spectrally resolved white-light interferometry: Comparative study of single-frame techniques," *Optics and Lasers in Engineering* 47, 1125-1130 (2009).
- 450"Uj cngf .P 0V0'Hkpcp.'LOF 0'I wkrm'H0'cpf "Y cz.'C0'oS wcpvkcxg'r'j cug'o letqueqr { 'qh'ctvkwrt'ej qpf tqe { 'vg'f { pco leu" "*****d { 'y kf g/hgrf 'f ki kcnlkwgthtqo gtx { .o'LODkqo gf 0Qr v0Ngw037"*4232+0'
- 460"Uj cngf .P 0V0'Ucwgty j kg.'N0N0'Vtwung { .I 0C0'cpf "Y cz.'C0'oS wcpvkcxg'o letqueqr { 'cpf'pcpqueqr { 'qh'ulemg'tgf" "*****dqjfqf 'egm't' gthtqo gf "d { 'y kf g/hgrf 'f ki kcnlkwgthtqo gtx { .o'LODkqo gf 0Qr v0Ngw038"*4233+0'